Microelectronics Journal 37 (2006) 204–212

Microelectronics Journal

www.elsevier.com/locate/mejo

Compensation and doping effects in heavily helium-radiated silicon for power device applications

R. Siemieniec [a,*], H.-J. Schulze [b], F.-J. Niedernostheide [b], W. Südkamp [c], J. Lutz [d]

[a] *Infineon Technologies Austria AG, Automotive and Industrial, Siemensstraße 2, A-9500 Villach, Austria*
[b] *Infineon Technologies AG, Automotive and Industrial, D-81726 Munich, Germany*
[c] *Infineon Technologies AG, Automotive and Industrial, D-81726 Munich, Germany*
[d] *Aktiv Sensor GmbH, Ruhlsdorfer Str. 95, Gebäude 4, D-14532 Stahnsdorf, Germany*
[e] *Faculty of Electrical Engineering and Information Technology, Technical University of Chemnitz, D-09107 Chemnitz, Germany*

Available online 4 November 2005

Abstract

The formation of defects modifying the effective doping concentration of helium-radiated p^+–n^-–n^+ and p^+–p^-–n^+ silicon diodes is analyzed as a function of the annealing temperature. After irradiation with helium at high energy levels and annealing at 220 °C, the probable formation of divacancy clusters increases the number of charged-acceptor states in a space-charge region. Capacitance-Voltage and Spreading-Resistance Profile measurements show that annealing at 350 °C results in the formation of an acceptor-like defect that deep level transient spectroscopy measurements suggest can be tentatively attributed to the V_2O or V_4/V_5 centre. Annealing at 430 °C results in the disappearance of the acceptor-like defect. Instead, pronounced donor formation in a range close to the penetration depth of the helium ions is observed. The influence of these effects on device characteristics is discussed.

Keywords: Lifetime control; Recombination centres; Compensation effects; Doping effects; Helium irradiation

1. Introduction

Irradiation techniques are widely used for carrier-lifetime control in bipolar power devices [1–7]. Electron irradiation results in a homogenous distribution of the generated recombination centres, while proton or helium irradiation generates inhomogeneous defect profiles.

It is well-known that proton irradiation followed by annealing in a temperature range between 250 and 500 °C leads to the formation of shallow donors. This effect limits the use of proton irradiation for carrier-lifetime control. The same effect can be used for the creation of deep *n*-doped regions [8], but sometimes the decreased carrier lifetime in the irradiated area limits such applications.

During helium irradiation, the formation of acceptor-like defects can result in a compensation of the doping concentration. A well-known double acceptor is the divacancy which, however, is only stable up to annealing temperatures of about 300 °C [9]. In this paper we first focus on doping and compensation effects of helium irradiation after annealing at temperatures ≥350 °C. A further increase of the annealing temperature causes the formation of donor-like centres while the recombination centres are vanishing. Finally, the possible formation of divacancy clusters in high-energy helium-radiated silicon annealed at 220 °C is discussed. Consequences for silicon devices are considered.

2. Experimental details

First, p^+–n^-–n^+ (Fig. 1) and p^+–p^-–n^+ (Fig. 2) test diodes were fabricated from FZ (floating zone)-grown silicon. The oxygen concentration in the conventionally prepared diodes was typically higher than $10^{16}\,cm^{-3}$. Helium irradiation was performed at room temperature with doses between 7×10^9 and $2.1\times10^{12}\,cm^{-2}$ and energies of 5.4 and 11.6 MeV, respectively. After irradiation, the samples were annealed at $T=350$ °C or $T=430$ °C in a nitrogen atmosphere for about 1 h. The doping of the n-type and p-type base material is $6\times10^{13}\,cm^{-2}$ and $3.3\times10^{13}\,cm^{-2}$, respectively.

Fig. 3 shows another test structure that consisted of a p–n^- junction and a parallel-connected thyristor [7]. The central p-region was surrounded by a p-ring that on one hand acted as

* Corresponding author. Tel.: +43 4242 3056876; fax: +43 4242 3056657.
E-mail addresses: ralf.siemieniec@infineon.com (R. Siemieniec), hans-joachim.schulze@infineon.com (H.-J. Schulze), franz-josef.niedernostheide@infineon.com (F.-J. Niedernostheide), wsuedkamp@aktiv-sensor.de (W. Südkamp), josef.lutz@etit.tu-chemnitz.de (J. Lutz).

0026-2692/$ - see front matter
doi:10.1016/j.mejo.2005.09.011

Symbols

P	Hole concentration	G	Generation rate
n	Electron concentration	R	Recombination rate
J_n	Electron current density	J_p	Hole current density
N_A^-	Acceptor density	N_D	Donor density
N_A	Ionized acceptor density	N_D^+	Ionized donor density
N_{TA}	Acceptor trap density	N_{TA}^-	Ionized acceptor trap density
N_{TD}	Donor trap density	N_{TD}^+	Ionized donor trap density
V_{TH}	Thermal voltage	E_T	Trap energy level
E_{TA}	Acceptor trap energy level	E_{TD}	Donor trap energy level
f_A	Fraction of occupied acceptor traps	f_D	Fraction of occupied donor traps
n_i	Intrinsic density	E_i	Intrinsic energy level
c_{nA}	Electron capture rate of acceptor traps	c_{pA}	Hole capture rate of acceptor traps
c_{nD}	Electron capture rate of donor traps	c_{pD}	Hole capture rate of donor traps
e_{nA}	Electron emission rate of acceptor traps	e_{pA}	Hole emission rate of acceptor traps
e_{nD}	Electron emission rate of donor traps	e_{pD}	Hole emission rate of donor traps
χ_{nA}	Electron entropy factor of acceptor traps	χ_{pA}	Hole entropy factor of acceptor traps
χ_{nD}	Electron entropy factor of donor traps	χ_{pD}	Hole entropy factor of donor traps
k_B	Boltzmann's constant	q	Elemental charge
t	Time	v_T	Thermal velocity v_T
ε_0	Absolute permittivity	ε_r	Relative permittivity
L_D	Diffusion length	ϕ	Potential

a field ring, and on other hand was part of the vertical n^+–p–n^-–p^+ structure, forming a thyristor. The p^+-layer, connecting the p–n^- diode and the concentric p-base of the thyristor, prevented the space-charge region from reaching the surface. Together with the electric field, which is always strongest at the position of maximum curvature of the p–n^- diode (when the p-layer is negatively biased with respect to the n^--layer), it was ensured that breakdown of the diode occurred in the bulk region. The n^--substrate was thick enough to ensure that the maximum electric field strength at the p–n^- junction met the avalanche ionization criterion before the field reached the anode p-layer. Thus the avalanche breakdown limited the maximum blocking voltage of the p–n^- diode. The thyristor connected in parallel with the diode protected the diode from damage due to breakdown. This was achieved by using the avalanche current to trigger the thyristor, which turned on when a certain avalanche current was exceeded. In this case, the voltage drop across the diode was reduced to less than 10 V. The typical avalanche breakdown voltage of the diodes investigated was about 5 kV at room temperature.

The applied irradiation energy of 24 MeV corresponds to a penetration depth of about 300 μm. The irradiated area comprises not only the junction area but also a part of the concentric p-ring (Fig. 3). Local irradiation was performed by irradiating the sample from the upper side through an aluminum mask with a pinhole. The irradiated samples were annealed for 4 h at about 220 °C. Three different helium doses were applied.

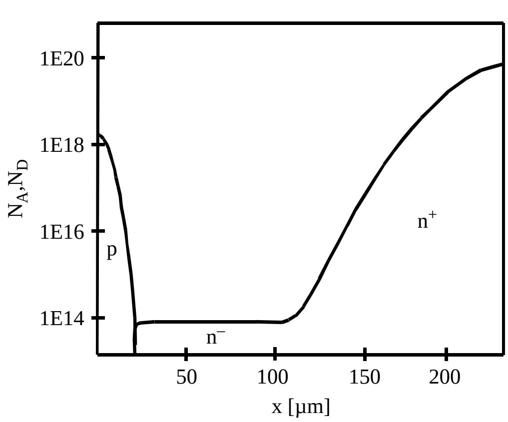

Fig. 1. Doping profile of the p^+–n^-–n^+ diodes ($N_{n-}=6\times10^{13}$ cm^{-3})

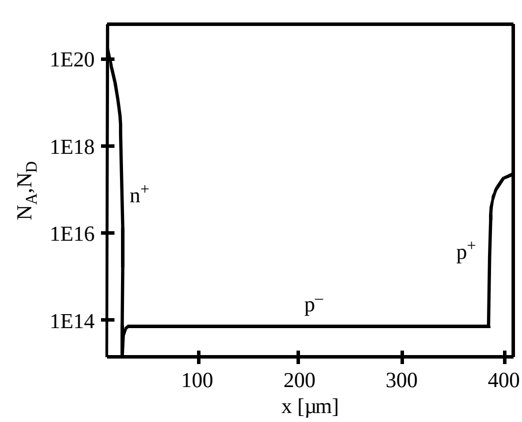

Fig. 2. Doping profile of the p^+–p^-–n^+ diodes ($N_{p-}=3.3\times10^{13}$ cm^{-3})